PROCEEDINGS OF SCIENCE

The TIGERISS Galactic Cosmic Ray Detector

Brian F. Rauch[a,*] **for the TIGERISS Collaboration**

[a] *Department of Physics and McDonnell Center for the Space Sciences, Washington University, St. Louis, MO 63130 USA*

E-mail: brauch@wustl.edu

The Trans-Iron Galactic Element Recorder for the International Space Station (TIGERISS) is a Galactic Cosmic Ray (GCR) detector being developed as a NASA Astrophysics Pioneers mission to launch to the ISS in 2027. TIGERISS has been assigned the Starboard Overhead X-Direction (SOX) location on the Columbus External Payload Facility (EPF) of the ISS. It will be the first instrument to measure the GCR elemental abundances from $_5$B to $_{82}$Pb over ~400 MeV/nucleon to ~10 GeV/nucleon with single element resolution. TIGERISS builds on the heritage of the TIGER and SuperTIGER stratospheric balloon-borne experiments flown from Antarctica and uses the proven combination of ionization (dE/dx) detectors with acrylic and silica aerogel Cherenkov-light-radiator ($\propto\beta$) detectors for charge and energy measurements. It improves on the predecessor instruments by using silicon strip detectors (SSDs) in place of both scintillating fiber hodoscopes for track reconstruction and large area scintillator detectors for dE/dx measurement and the instrument trigger. The superior charge resolution ($\sigma_Z < 0.25$) and signal linearity over the full dynamic range of the TIGERISS SSDs have been demonstrated in CERN beam tests. TIGERISS will also use silicon photomultipliers (SiPMs) instead of photomultiplier tubes (PMTs) to forego the need for high voltage (HV) and for the more compact Cherenkov detector readout needed to maximize the instrument geometry within the payload envelope. This enables an instrument geometry factor of 1.21 m^{2}sr that will allow TIGERISS in one year to observe GCR statistics comparable to those observed in the first 55-day SuperTIGER flight over their common measurement range without the systematics from atmospheric propagation corrections. With the possibility of extended observations, TIGERISS will test models of GCR origins, including their source environments and acceleration mechanisms. In measuring GCRs over nearly the entirety of the s-process and r-process (slow and rapid) neutron capture processes and the rp-process rapid-proton capture process of heavy-element nucleosynthesis, TIGERISS will make a significant contribution to the wider multi-messenger effort to determine the relative contributions of supernovae (SNe) and Neutron Star Merger (NSM) events.

39th International Cosmic Ray Conference (ICRC2025)
15–24 July 2025
Geneva, Switzerland

*Speaker

†TIGERISS supported by NASA under cooperative agreement 80NSSC22M0299, the McDonnell Center for the Space Sciences, and the Peggy and Steve Fossett Foundation

PoS(ICRC2025)118

1. Introduction

1.1 Motivation

The Trans-Iron Galactic Element Recorder for the International Space Station (TIGERISS) has a planned launch in 2027 and will provide the best data set yet for ultra-heavy Galactic cosmic ray (UHGCR) abundances. This will enable TIGERISS to address questions about the grand cycle of matter in the Galaxy, including the nature of the astrophysical reservoirs of nuclei at the Galactic cosmic-ray (GCR) sources (GCRSs) and the mechanisms by which nuclei are drawn from the reservoirs and injected into the GCR accelerators. TIGERISS will contribute to the multi-messenger search for sources of r-process neutron capture synthesis of the heavier elements. Previous GCR measurements through $_{40}$Zr point to a source with a major contribution from OB associations, with a composition primarily of older interstellar media (ISM) with fresh nucleosynthetic products of younger stars mixed in and acceleration by shock waves from stellar deaths. The GCRs help energize Galactic magnetic fields and feed back into the process of new star formation, as depicted in Fig. 1, a picture has been pieced together over many years from evidence gleaned from measurements of elemental and isotopic composition, energy spectra, and gamma rays emitted in cosmic-ray interactions with the ISM.

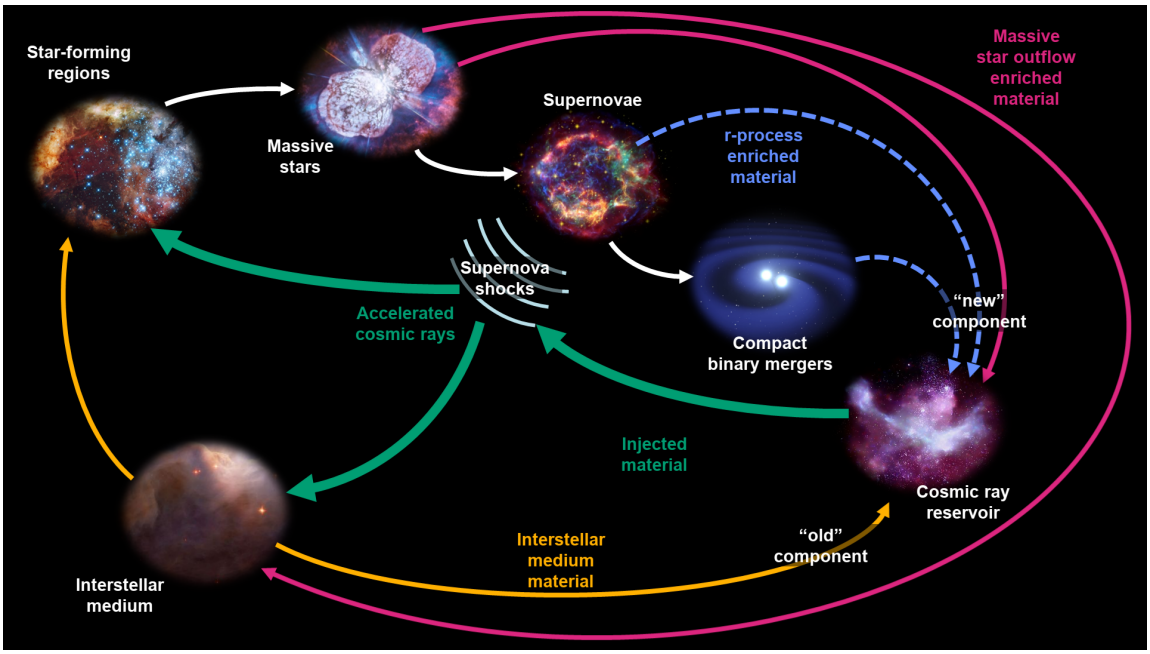

Figure 1: Cycle of matter in the Galaxy. Star forming regions create massive stars that inject matter into the interstellar medium via stellar wind and supernova shocks. Many of the heaviest nuclei are produced in the most energetic processes: supernova and NSM.

For many years cosmic-ray acceleration and the r-process neutron capture nucleosynthesis of the heavier elements in the cycle shown in Fig. 1 were thought to occur predominantly if not exclusively in supernovae. More recent multi-messenger observations of kilonovae involving gravitational wave [1] and broader electromagnetic spectral observations [2] have provided strong evidence supporting the model of binary neutron star merger nucleosynthesis of the heaviest r-process elements. The

first single-element resolution UHGCR measurements above $_{40}$Zr by SuperTIGER indicate that something is missing from the OB association GCRS model with a major contribution from OB associations and preferential acceleration of elements condensed on dust grains [3–6]. TIGERISS will investigate the elemental composition of the heavier UHGCRs with unprecedented resolution to address these scientific questions, which are discussed in more detail in [7].

1.2 Status

TIGERISS belatedly passed the first key decision point in late August of 2024. It was finally assigned an ISS external payload location on December 18, 2024. The TIGERISS Payload Integration Management (PIM) kickoff meeting was January 22, 2025, at which point the TIGERISS team began to have access to payload requirements, and at present we are still working to establish non disclosure agreements (NDAs) with prospective launch providers to have environmental and other launch vehicle requirements to design and test to. The critical design review (CDR) is planned for the middle of January, 2026. The funding outlook for the next fiscal year is unclear.

2. TIGERISS Instrument

The proposed TIGERISS location on the International Space Station (ISS) was the Japan Aerospace Exploration Agency (JAXA) Japanese Experiment Module (JEM) "Kibo" Exposed Facility Unit 10 (EFU10), but this location was unavailable when TIGERISS was selected. We were required to study payload configurations for all possible external attachment locations, and were developing models for JEM-EFU6 and EFU7 and the European Space Agency (ESA) Columbus Laboratory external payload Starboard Overhead X-Direction (SOX) location. None of the zenith facing National Aeronautics and Space Administration (NASA) EXpedite the PRocessing of Experiments to the Space Station (ExPRESS) Logistics Carrier (ELC) locations are expected to be available. A technical model of the Columbus SOX configuration for the 10x9 SSD configuration is shown in Fig. 2a, and a finite element model stress analysis is shown in Fig. 2b. We have now descoped to a 9x9 SSD configuration, reducing the instrument geometry factor from 1.21 m^2 sr to 1.06 m^2 sr.

An expanded view of the TIGERISS SOX model is shown in Fig. 2c. TIGERISS will use three basic detector subsystems to unambiguously measure the charge of all GCRs from $_5$B to $_{82}$Pb with energies greater than ~0.2 GeV/nucleon. TIGERISS uses crossed pairs of SSD layers at the top and bottom of the instrument stack to measure both particle trajectory and ionization energy deposits (dE/dx), replacing the scintillating optical fiber hodoscopes and scintillator detectors used in the TIGER family of stratospheric balloon-borne instruments. An expanded view of a SSD module is shown in Fig. 2d. Two Cherenkov detectors measure nuclear charge (Z) and velocity (β): C0 with a silica aerogel radiator over C1 with an acrylic radiator, with an expanded view of the acrylic detector shown in Fig. 2e.

CERN beam tests of SSD detectors have demonstrated single element resolution ($\sigma_Z \leq 0.24$) down to ~200 MeV/nucleon for Z $\geq$ 5 [8]. These detectors improve on the scintillators used in TIGER/SuperTIGER [9, 10] in in terms of resolution and linearity of signal response with Z, as they do not suffer from saturation effects. The charge assignment method using the multiple SSD dE/dx measurements independently and with Cherenkov signals above their thresholds complements the

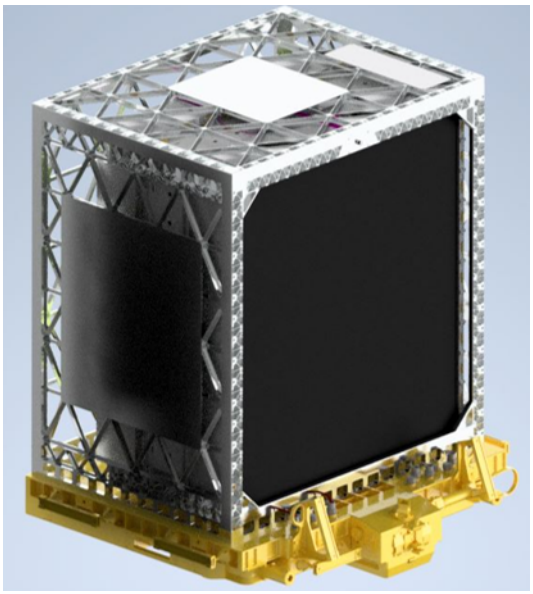

Figure 2(a): Columbus SOX TIGERISS payload technical model.

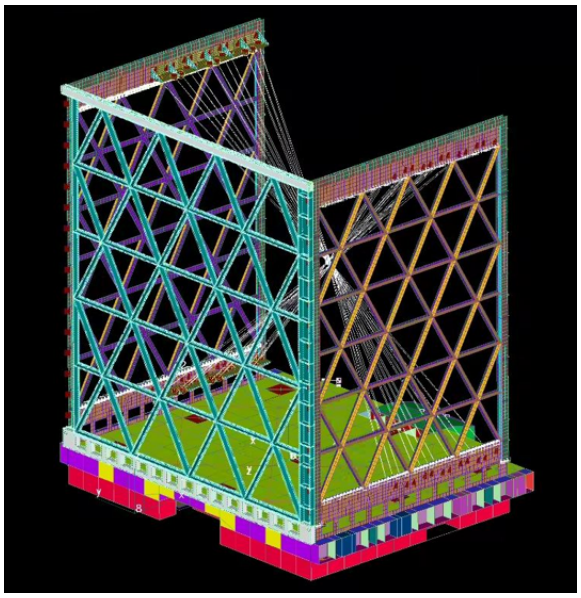

Figure 2(b): Finite element model analysis of SOX payload structure.

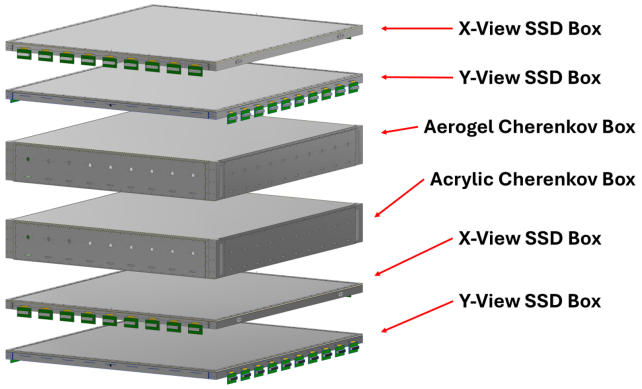

Figure 2(c): Expanded view of the standard TIGERISS instrument technical model.

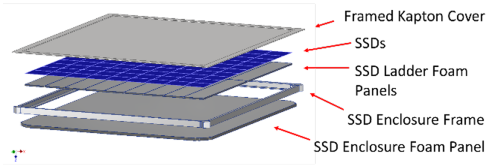

Figure 2(d): SSD expanded view.

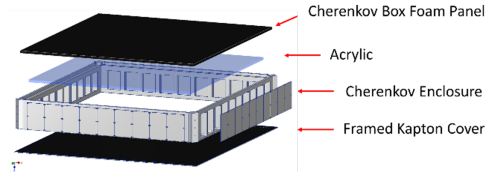

Figure 2(e): Cherenkov detector expanded view.

acrylic Cherenkov (n=1.49, $\beta > 0.67$, KE $\geq$ 325 MeV/nucleon) versus aerogel Cherenkov (n=1.05, $\beta > 0.95$, KE $\geq$ 2.12 GeV/nucleon) technique successfully demonstrated on TIGER/SuperTIGER for energies above the aerogel threshold [9, 10]. TIGERISS will be capable of measuring elements to the end of the periodic table, but statistics will limit it to Z ~83 for any foreseeable ISS exposure duration.

3. Science Objectives

3.1 Ultra-Heavy Galactic Cosmic Rays

The GCRs and the Solar System (SS) represent two directly measurable samples of Galactic matter, with the few million year old GCRs being far younger than the ~4.6 billion year old SS sample of the Galactic ISM. A comparison of the relative abundances of GCRs with energies of ~2

GeV/nucleon [5, 9, 11–13] to those of SS [14] from $_{1}$H to $_{56}$Ba normalized to $_{14}$Si = 1 is shown in Fig. 3. In the GCRs $_{26}$Fe is ~5×10^{3} times less abundant than $_{1}$H, and the UHGCRs are in turn ~10^{5} times less abundant than $_{26}$Fe. The major differences between the GCR and SS abundances seen below $_{26}$Fe are generally understood to arise from elemental acceleration efficiencies of the GCR and nuclear fragmentation between the GCRS and detection.

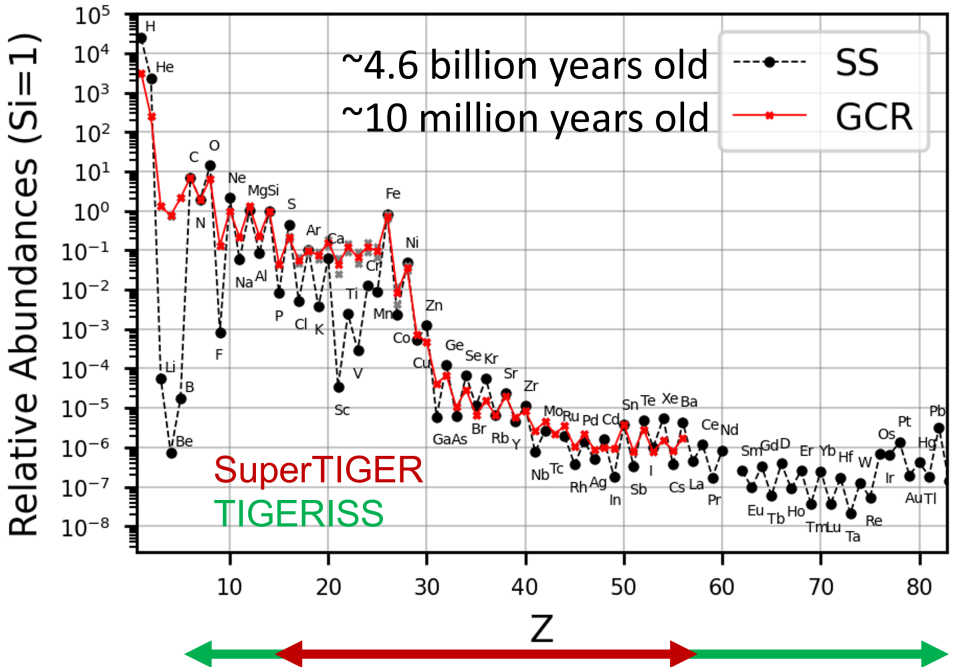

Figure 3: Solar System (SS) [14] and Galactic cosmic-ray (GCR) relative abundances at 2 GeV/nuc. The red line depicts average GCR data, sourced for 1≤Z≤2 from [11], Z=3 from [12], 4≤Z≤28 from [13], and 16≤Z≤56 from [3] normalized to $_{14}$Si. Grey dots depict overlapping measurements from [13] and [3].

Figure 3 shows GCR abundances through $_{56}$Ba that have been measured with single-element resolution, with the UHGCRs from SuperTIGER [5]. UHGCR measurements through $_{40}$Zr by TIGER [9], SuperTIGER [10], CALET [15], and ACE-CRIS [16] together with ACE-CRIS isotopic measurements ($^{22}_{10}$Ne [17], $^{56}_{26}$Fe [18]) suggest that the GCRS is enhanced in material produced in massive stars ejected by solar winds and in supernovae. Figure 4a shows that for GCR observations up to ~$_{40}$Zr corrected for propagation effects to GCRS abundances, and with the refractory elements that more readily condense on interstellar dust grains are preferentially accelerated over volatile elements that are less likely to, and that injection into the GCRs for both refractory and volatile elements follow a charge dependence consistent with their grain sputtering cross sections ($\propto Z^{2/3}$) [19]. This suggests that a significant fraction of the cosmic rays originate in OB associations where material from earlier generations of massive stars (~20%) mixes with ISM (~80%) with SS composition and is accelerated by subsequent supernovae.

The more recent SuperTIGER analysis extended the UHGCR measurements from the first flight up to $_{56}$Ba [3, 4, 6], showing that above $_{40}$Zr volatile elements are enhanced to roughly the same degree as the refractories. The breakdown of the OB association GCRS model for UHGCR elements where MSM abundances are significantly enhanced over SS with a stron s-

process component suggests the possibility of another r-process source component other than ISM and fresh MSM, such as neutron star merger (NSM) material. The breakdown in the preferential acceleration of refractory elements may also result from the MSM component being the hot rarefied OB association bubbles and the ISM being mainly the denser cool shell where the volatile elements may condense onto dust grains at a level comparable to the refractory elements.

TIGERISS observations will help determine the relative amounts of nucleosynthesis by s- and r-process neutron capture in the UHGCRs and the relative contributions of massive stars and other nucleosynthesis sources. Figure 4b gives a deconvolution model of the r- and s- neutron-capture processes as a function of atomic number while also showing the volatile and refractory breakdown. TIGERISS can disentangle the contributions from GCRS components and preferential acceleration by measuring UHGCR abundances through $_{82}$Pb. In only one year significant measurements will be made of the more abundant dominant s-process ($_{50}$Sn and $_{56}$Ba) and r-process ($_{52}$Te, $_{54}$Xe) elements. Three of these are volatile ($_{50}$Sn, $_{52}$Te and $_{54}$Xe) and only one is refractory ($_{56}$Ba), which will allow TIGERISS to disentangle the impact of acceleration efficiency to determine the relative contributions of the r- and s-process to the GCRS in the $_{50}$Sn - $_{56}$Ba group.

3.2 Energy Spectra

TIGERISS will also measure energy spectra of the more abundant elements between $_5$B to $_{28}$Ni from above the trigger threshold for the bottom SSD detector to where the silica aerogel Cherenkov signal plateaus, near $\beta = 1$ at ~10 GeV/nucleon. These measurements will complement those by SuperTIGER other instruments, including AMS-02 and CALET already on the ISS, and the ACE-CRIS and DAMPE satellite instruments. The comparatively large geometry factor of TIGERISS will make it a sensitive probe for temporally variant spectral features that could arise from phenomena like microquasars.

4. Predicted TIGERISS Abudance Observations

TIGERISS measurements for the current SOX instrument configuration in the ~1 year on the ISS under the original NASA Astrophysics Pioneers Program proposal will address important science goals. Figure 5 gives predicted one year TIGERISS measurements for the proposal JEM-EF model 1-year statistics (pink), Columbus SOX 1-year statistics (black), and Columbus SOX

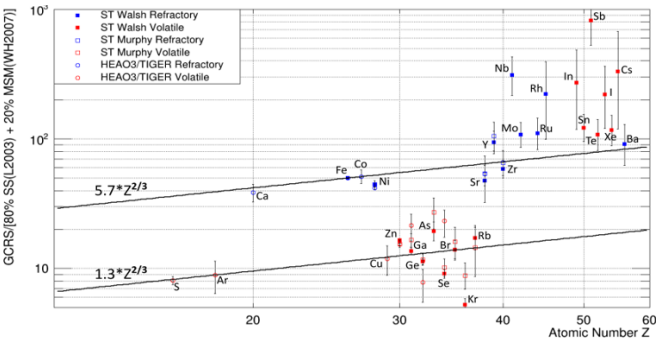

Figure 4(a): SuperTIGER results through $_{56}$Ba showing that the OB association GCRS model fails above $_{40}$Zn.

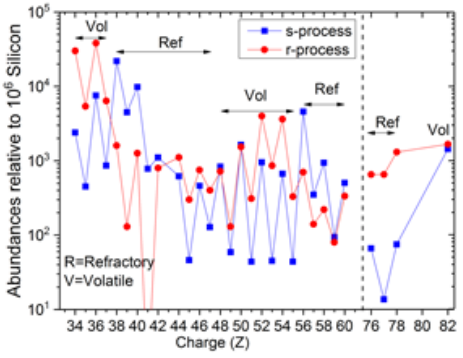

Figure 4(b): Model of s- and r-process composition showing refractory and volatile elements.

3-year statistics (blue) configurations [20] compared with those from the first SuperTIGER flight (red) [3–6]. The predicted abundances are for average solar modulation, and the level of solar modulation has been found not to have a strong impact on the TIGERISS UHGCR measurements due to geomagnetic screening in the ISS orbit.The expected one-year statistics are comparable to or better than those of SuperTIGER in their common dynamic range and will have both superior charge resolution and dynamic range. The TIGERISS predictions between $_{40}$Zr and $_{60}$Nd are based on the assumed 20% odd/80% even splitting of charge pairs measured by HEAO-3-C2 [21], which agree reasonably with the SuperTIGER measurements, and abundances of elements in HEAO-3-C2 charge groups above $_{60}$Nd are scaled by SS abundances. Major differences between SuperTIGER and predicted TIGERISS abundances include unstable $_{43}$Tc enhanced at balloon altitudes by secondary production and the elements around $_{48}$Cd at the high- and low-gain transition in SuperTIGER makes their lower measured values suspect. TIGERISS measurements through $_{56}$Ba will check the SuperTIGER results, while also probing the r- and s-process contributions to the UHGCR in the $_{50}$Sn - $_{56}$Ba group.

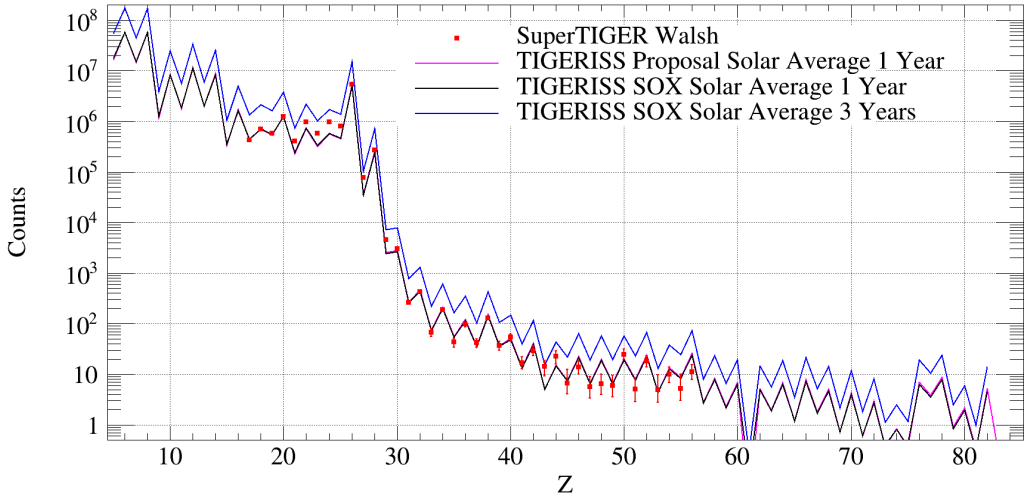

Figure 5: Predicted abundances measured by TIGERISS after 1 and 3 years of operation [20] compared to those measured by SuperTIGER over its 55 day long-duration-balloon flight [3–6].

5. Conclusions

The TIGERISS instrument comprised of SSD and silica aerogel and acrylic Cherenkov detectors make the first single-element resolution GCR measurements from $_5$B to $_{82}$Pb. It will probe the GCRS and the mechanisms that inject material into accelerators. In one year of measurements TIGERISS will check the SuperTIGER results with reduced systematic uncertainties and double the total statistics of the UHGCR measurements that conflict with the leading OB association GCRS model. TIGERISS will also make the first preliminary single-element UHGCR measurements from $_{56}$Ba to $_{82}$Pb and make more significant observations if operations are extended. It will probing the relative contributions of r- and s-process neutron capture sources to the GCRs and contribute to the multi-messenger effort to determine the sources of r-process nucleosynthesis.

6. References

[1] B. P. Abbott *et al.*, "Gw170817: Observation of gravitational waves from a binary neutron star inspiral," *Phys. Rev. Lett.*, vol. 119, p. 161101, Oct 2017.

[2] B. P. Abbott *et al.*, "Multi-messenger observations of a binary neutron star merger," *The Astrophysical Journal*, vol. 848, p. L12, oct 2017.

[3] N. E. Walsh, *SuperTIGER Elemental Abundances for the Charge Range* $41 \leq Z \leq 56$. PhD thesis, Washington University in St. Louis, 2020.

[4] N. E. Walsh *et al.*, "SuperTIGER Abundances of Galactic Cosmic Rays for the Atomic Number (Z) Interval 30 to 56," in *Proceedings of 37th International Cosmic Ray Conference — PoS(ICRC2021)*, vol. 395, p. 118, 2021.

[5] N. E. Walsh *et al.*, "SuperTIGER instrument abundances of galactic cosmic rays for the charge interval $41 \leqslant Z \leqslant 56$," *Advances in Space Research*, vol. 70, pp. 2666–2673, Nov. 2022.

[6] N. E. Walsh, "SuperTIGER Abundances of Galactic Cosmic Rays for the Atomic Number (Z) Interval 40 to 56," in *Proceedings of 38th International Cosmic Ray Conference — PoS(ICRC2023)*, vol. 444, p. 053, 2023.

[7] W. V. Zober, B. F. Rauch, *et al.*, "Science Objectives and Goals of the TIGERISS mission," in *Proceedings of 38th International Cosmic Ray Conference — PoS(ICRC2023)*, vol. 444, p. 144, 2023.

[8] J. F. Krizmanic *et al.*, "HNX/SuperTIGER Silicon Strip Detector Response to Nuclei in Lead Primary and Fragmented Test Beams," in *36th International Cosmic Ray Conference (ICRC2019)*, vol. 36 of *International Cosmic Ray Conference*, p. 94, July 2019.

[9] B. F. Rauch *et al.*, "Cosmic Ray Origin in OB Associations and Preferential Acceleration of Refractory Elements: Evidence from Abundances of Elements $_{26}$Fe through $_{34}$Se," *The Astrophysical Journal*, vol. 697, no. 2, pp. 2083–2088, 2009.

[10] R. P. Murphy *et al.*, "Galactic Cosmic Rays Origins and OB Associations: Evidence from SuperTIGER Observations of Elements $_{26}$Fe through $_{40}$Zr," *The Astrophysical Journal*, vol. 831, no. 2, p. 148, 2016.

[11] T. Sanuki *et al.*, "Precise Measurement of Cosmic-Ray Proton and Helium Spectra with the BESS Spectrometer," *The Astrophysical Journal*, vol. 545, no. 2, pp. 1135–1142, 2000.

[12] M. Aguilar *et al.*, "Isotopic Composition of Light Nuclei in Cosmic Rays: Results from AMS-01," *The Astrophysical Journal*, vol. 736, p. 105, Aug. 2011.

[13] J. J. Engelmann *et al.*, "Charge Composition and Energy Spectra of Cosmic-Ray Nuclei for Elements from Be to Ni. Results from HEAO-3-C2," *Astronomy & Astrophysics*, vol. 233, pp. 96–111, 1990.

[14] K. Lodders, "Solar System Abundances and Condensation Temperatures of the Elements," *The Astrophysical Journal*, vol. 519, pp. 1220–1247, 2003.

[15] W. V. Zober and The Calet Collaboration, "Detected Abundances of Nuclei Relative to $_{26}$Fe for Elements $_{14}$Si through $_{44}$Ru with CALET on the International Space Station," *ApJ*, vol. 988, p. 148, Aug. 2025.

[16] W. R. Binns *et al.*, "Elemental Source Composition Measurements and the Origin of Galactic Cosmic Rays," in *36th International Cosmic Ray Conference (ICRC2019)*, vol. 36 of *International Cosmic Ray Conference*, p. 36, July 2019.

[17] J. C. Higdon and R. E. Lingenfelter, "OB Associations, Supernova-Generated Superbubbles, and the Source of Cosmic Rays," *The Astrophysical Journal*, vol. 628, pp. 738–749, 2005.

[18] W. R. Binns *et al.*, "Observation of the ^{60}Fe nucleosynthesis-clock isotope in galactic cosmic rays," *Science*, vol. 352, pp. 677–680, May 2016.

[19] R. E. Lingenfelter, "The Origin of Cosmic Rays: How Their Composition Defines Their Source and Sites and the Process of Their Mixing, Injection, and Acceleration," *The Astrophysical Journal Supplement Series*, vol. 245, p. 30, 2019.

[20] B. F. Rauch, W. V. Zober, *et al.*, "Modeling Expected TIGERISS Observations," in *Proceedings of 38th International Cosmic Ray Conference — PoS(ICRC2023)*, vol. 444, p. 172, 2023.

[21] W. R. Binns *et al.*, "Abundances of Ultraheavy Elements in the Cosmic Radiation: Results from HEAO 3," *The Astrophysical Journal*, vol. 346, pp. 997–1009, 1989.

Full Author List: TIGERISS Collaboration

H. Allen, [1] R. F. Borda, [2] R. G. Bose, [3] D. L. Braun, [3] J. Calderon, [4] Z. Campbell, [5] N. W. Cannady, [6] R. M. Caputo, [6] M. Clark, [7] J. Coldsmith, [8] S. Coutu, [1] G. A. de Nolfo, [9] T. Forstmeier, [1] M. Fratta, [5] P. Ghosh, [2,6,10] S. Graham, [8] S. Jones, [4] J. F. Krizmanic, [6] W. Labrador, [3] L. Lisalda, [3] J. V. Martins, [2] M. P. McPherson, [7] J. G. Mitchell, [9] J. W. Mitchell, [6] S. I. Mognet, [1] A. Moiseev, [11,6,10] T. L. Ng, [5] S. Nutter, [4] N. Osborn, [3] M. Pant, [4] I. M. Pastrana, [3] D. Radomski, [3] B. F. Rauch, [3] H. Salmani, [7] M. Sasaki, [11,6,10] G. E. Simburger, [3] S. Smith, [7] H. A. Tolentino, [7] Y. Tufail, [5] D. Washington, [1] T. Widmyer, [5] L. Williams, [8] W. V. Zober, [3]

[1] Pennsylvania State University
[2] University of Maryland, Baltimore County
[3] Department of Physics and McDonnell Center for the Space Sciences, Washington University in St. Louis
[4] Northern Kentucky University
[5] NASA Wallops Flight Center
[6] NASA Goddard Space Flight Center Astrophysics Science Division
[7] Howard University
[8] NASA Goddard Space Flight Center
[9] NASA Goddard Space Flight Center, Heliophysics Science Division
[10] Center for Research and Exploration in Space Sciences and Technology II
[11] University of Maryland, College Park